ACS chemical biology

ARTICLE

Regioisomeric SCFA Attachment to Hexosamines Separates Metabolic Flux from Cytotoxicity and MUC1 Suppression

Udayanath Aich, Christopher T. Campbell, Noha Elmouelhi, Christopher A. Weier, S.-Gopalan Sampathkumar, Sean S. Choi, and Kevin J. Yarema*

Department of Biomedical Engineering, The Johns Hopkins University, Clark Hall 106A, 3400 N. Charles St., Baltimore, Maryland 21218

ABSTRACT Chemical biology studies, exemplified by metabolic glycoengineering experiments that employ short chain fatty acid (SCFA)-hexosamine monosaccharide hybrid molecules, often suffer from off-target effects. Here we demonstrate that systematic structure–activity relationship (SAR) studies can deconvolute multiple biological activities of SCFA-hexosamine analogues by demonstrating that triacylated monosaccharides, including both *n*-butyrate- and acetate-modified ManNAc analogues, had dramatically different activities depending on whether the free hydroxyl group was at the C1 or C6 position. The C1-OH (hemiacetal) analogues enhanced growth inhibition in MDA-MB-231 human breast cancer cells and suppressed expression of MUC1, which are attractive properties for an anticancer agent. By contrast, C6-OH analogues supported high metabolic flux into the sialic acid pathway with negligible growth inhibition or toxicity, which are desirable properties for glycan labeling in healthy cells. Importantly, these SAR were general, applying to other hexosamines (*e.g.*, GlcNAc) and non-natural sugar "scaffolds" (*e.g.*, ManNLev). From a practical standpoint, the ability to separate toxicity from flux will facilitate the use of MOE analogues for cancer treatment and glycomics applications, respectively. Mechanistically, these findings overturn the premise that the bioactivities of SCFA-monosaccharide hybrid molecules result from their hydrolysis products (*e.g.*, *n*-butyrate, which acts as a histone deacetylase inhibitor, and ManNAc, which activates sialic acid biosynthesis); instead the SAR establish that inherent properties of partially acylated hexosamines supersede the cellular responses supported by either the acyl or monosaccharide moieties.

*Corresponding author,
kyarema1@jhu.edu.

Received for review December 31, 2007
and accepted February 17, 2008.

Published online March 14, 2008

10.1021/cb7002708 CCC: $40.75

Metabolic glycoengineering exploits the substrate permissivity of glycosylation pathways to biosynthetically incorporate non-natural monosaccharides into the glycans of living cells (Figure 1, panel a). This technique was pioneered by the Reutter group who used *N*-acetyl-D-mannosamine (ManNAc) analogues bearing extended alkyl chains to install the corresponding *N*-acyl modified sialosides into cell surface glycans (*1*). In the past decade, metabolic glycoengineering has built on this foundation by branching out in two directions. First, the Bertozzi group incorporated bioorthogonal chemical functionalities, such as the ketone (*2*) and azide (*3*) groups not normally found in the glycocalyx, into the *N*-acyl groups of ManNAc analogues. Second, monosaccharide vehicles have extended beyond sialic acid to now include analogues of *N*-acetyl-D-galactosamine (GalNAc), *N*-acetyl-D-glucosamine (GlcNAc), and fucose (*4*). Together, these developments, which increase both the scope of chemical functional groups and the diversity of target glycans, combined with increasingly versatile chemoselective ligation strategies exemplified by "click chemistry" (*5, 6*), have dramatically expanded the ability to manipulate and exploit glycosylation in living cells and animals.

Although there are many potential applications for metabolic glycoengineering with important research, bioindustrial, and biomedical significance, such as inhibition of viral binding (*7*), metabolic labeling useful for glycomics (*8, 9*), control of stem cell biology (*10*), and nascent cancer treatment strategies (*11, 12*), the development of this field has been hindered by the inefficient membrane uptake of hydrophilic monosaccharide analogues. As a consequence, millimolar concentrations (often 50 mM or higher) of "free hydroxyl" analogues

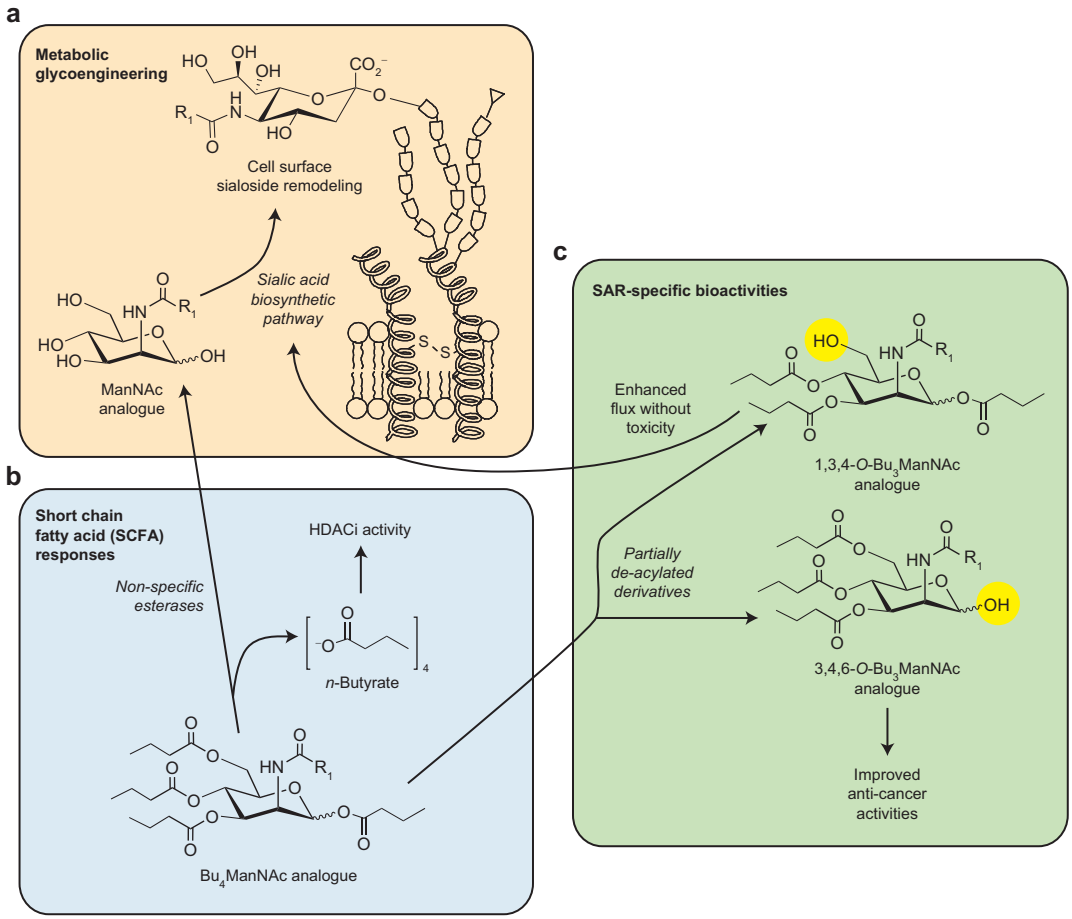

Figure 1. SCFA-hexosamine design for glycoengineering. a) Metabolic glycoengineering was pioneered by using ManNAc analogues to replace natural sialosides on the cell surface with their "R_1"-modified counterparts. b) SCFA-hexosamine hybrid molecules, illustrated by Bu_4ManNAc analogues (*e.g.*, 1 or 12 shown in later figures), generate free SCFAs that have HDACi activity and feed the core sugar into the targeted glycosylation pathway. c) Triacylated derivatives of Bu_4ManNAc (*e.g.*, 3, 4, and 13), which can be generated enzymatically or by chemical synthesis, have dramatically different bioactivities if the SCFA moiety is absent from the C1 or the C6 position. Of note, similar SAR apply to acetylated ManNAc (*e.g.*, 5–7 and 11) and to GlcNAc (*e.g.*, 8–10) analogues.

were required for robust surface display of glycoengineered epitopes (*13*). A substantial improvement in metabolic efficiency was achieved by the peracylation of monosaccharide analogues (or disaccharides used as "decoys" for mucin production (*14*)) with ester-linked short chain fatty acids (SCFAs) (*15–17*). Quantitatively, sialic acid production in cells incubated with peracetylated ManNAc was ~600-fold more efficient than in cells incubated with natural ManNAc, and conjugation with *n*-butyrate resulted in an increase of ~2,100-fold (*18*).

Despite the increase in efficiency for acetate- or *n*-butyrate-derivatized monosaccharides, experiments with these hybrid molecules were complicated by the SCFA. To explain briefly, nonspecific esterases must hydrolyze the SCFA from the "core" monosaccharide to allow the sugar to enter the targeted pathway. For peracylated ManNAc to be converted to sialic acid, for example, the biochemical steps involved require a free hydroxyl at the C1, C3, and C6 positions (*19*). Moreover, a lack of acetyl groups in surface sialosides incubated with the peracetylated glycolyl derivative of ManNAc (*20*) indicates

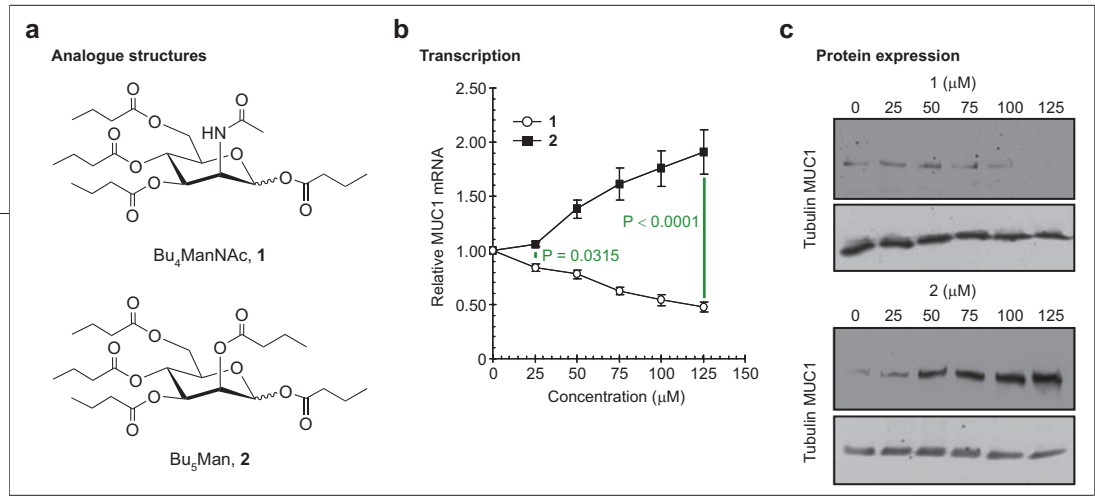

Figure 2. MUC1 is up-regulated by 1 and down-regulated by 2 in MDA-MB-231 cells. a) Structures of 1 and 2. b) qRT-PCR analysis (error bars indicate SEM, $n = 9$; *P* values were calculated with GraphPad Software and show statistical differences between 1 and 2 at concentrations as low as 25 μM). c) Western analysis of MUC1 levels; similar blots were obtained in five experiments.

that hydrolysis at the C4 position also occurs. Once liberated from the core sugar (Figure 1, panel b), SCFAs have many biological activities of their own; for example, acetate, propionate, and *n*-butyrate each function as histone deacetylase inhibitors (HDACi (*21*)) and elicit unique signatures of altered gene expression (*22*).

The combination of glycan- and SCFA-specific activities of sugar analogues used in metabolic glycoengineering opens new possibilities for these molecules but also introduces a tangled web of biologic responses difficult to deconvolute and potentially impossible to control toward a defined end. Nascent efforts to apply the multifaceted effects of SCFA-ManNAc analogues for cancer treatment illustrate this conundrum. First, because peracetylated ManNAc analogues such as Ac_4ManNLev or perbutanoylated compounds such as Bu_4ManNAc (*23*) are effective inducers of apoptosis, efforts arose to exploit this toxicity to kill cancer cells (*11*). Second, glycan labeling and cytotoxicity can work hand in hand, for example, abiotic "R_1" groups (Figure 1, panel a) can function as "tags" for chemoselective ligation to therapeutic (*2*) and diagnostic agents (*15*) or as neo-epitopes for passive immune-based therapeutic strategies (*12, 24*). Despite multipronged anticancer prospects, other aspects of the hybrid molecules cause concern, however. For example, increased sialic acid production from ManNAc-based analogues may, based on the compelling evidence for multiple roles for sialic acid in metastasis (*25*), increase the invasive potential of cancer cells, thus offsetting any benefits realized from surface "tags" or enhanced apoptosis.

Clearly, the complex web of biological activities arising from SCFA-hexosamine analogues provides obstacles for the practical applications of metabolic glycoengineering. In another example, glycomic labeling applications in healthy cells require high flux into the targeted glycosylation pathway. Therefore, because *n*-butyrate is several-fold more effective at increasing flux than acetate (*23*), this SCFA would, at first, appear ideal for labeling applications. However, *n*-butyrate also blocks replication (*11*), and because robust cell growth is linked to high flux (*18*), the growth inhibitory properties of this SCFA counter the benefits of increased cellular uptake. In practice, these counteracting forces result in a narrow concentration range for optimal metabolic flux (*e.g.*, flux increases rapidly between 75 and 100 μM for Bu_4ManNAc but then precipitously declines above 125 μM due to cytotoxicity (*11*)); flux also depends on cell density (*23*), making *in vitro* optimization laborious and *in vivo* experiments almost impossible to design rationally.

The purpose of this report is to describe design principles that allow metabolic flux supported by SCFA-hexosamines to be separated from the growth inhibition and toxicity engendered by this class of molecules. Consequently, the SAR described in this report, based on the regiospecific placement of SCFA groups on a hexosamine "scaffold" (Figure 1, panel c), which permit promising anticancer properties to be maintained separate from metabolic flux through glycosylation pathways, promise to facilitate the development of cancer therapies. Conversely, complementary SAR that facilitate metabolic flux and surface labeling without concomitant toxicity will propel the development of metabolic glycoengineering in healthy cells and living animals.

RESULTS AND DISCUSSION

Metabolism of SCFA-Hexosamine analogues. The SAR outlined in this paper that decouple the multiple and often conflicting biological responses to SCFA-hexosamine analogues used in metabolic glycoengineering were inspired by the *in vitro* anticancer properties of perbutanoylated ManNAc (Bu_4ManNAc, **1**; Figure 2,

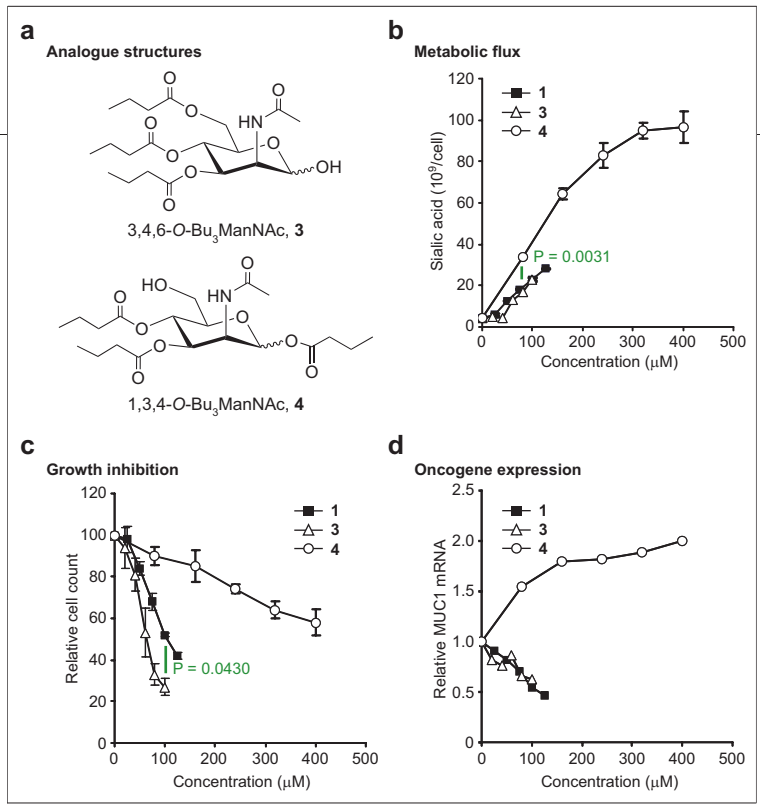

Figure 3. Bioactivities of tributanoylated ManNAc analogues 3 and 4 in MDA-MB-231 cells. a) Structures of 3 and 4 (1 is shown in Figure 2). b) Metabolic flux indicated by sialic acid production measured by the periodate resorcinol assay with *P* values showing that 4 is more efficient at supporting sialic acid levels at >80 μM. c) Growth inhibition after 3 days showing a significant difference between 3 and 4 at 100 μM; in panels b and c, error bars indicate SEM, $n \geq 3$. d) MUC1 mRNA levels were determined by qRT-PCR and data for a representative experiment are shown (the experiment was repeated three times with comparable results). In general, tests were not continued once analogue levels reached toxic concentrations, and consequently different concentration ranges were used for the data plotted on each graph.

panel a). This compound elicits *in vitro* growth inhibition for 3–5 days after analogue exposure, apoptosis over the ensuing two weeks (*11*), and suppression of the pro-invasive oncogene mucin 1 (MUC1). On the basis of these promising *in vitro* results, which exceed clinically tested SCFA-carbohydrate hybrid molecules such as perbutanoylated mannose (Bu_5Man, **2**; Figure 2, panel a) or tributyrin (tributanoylated glycerol) (*26*), we considered the *in vivo* prospects for **1** and noted that removal of one *n*-butyrate improved prospects for oral availability predicted by Lipinski rule-of-5 properties (*27*). Moreover, the absence of one SCFA provides peracylated hexosamines with greater amphiphilicity, which increases solubility in tissue culture medium, enhances membrane permeability, and facilitates cellular uptake. On the basis of these factors, we anticipated that tributanoylated ManNAc analogues would have superior cell-level (as well as pharmacologic, beyond the scope of this study) properties and began testing cell responses to **3** (tributanoylated ManNAc lacking the SCFA at the C1 position; Figure 3, panel a) and the regioisomer **4** (tributanoylated ManNAc with the free hydroxyl at C6).

Three end points were selected to evaluate the biological activities of the partially acylated ManNAc analogues. The first two metrics were based on known responses to hydrolysis products of **1**, specifically, growth inhibition consistent with the HDACi effects of *n*-butyrate (*11*) and activation of sialic acid biosynthesis by ManNAc (*23*). As a third end point, we were interested in evaluating MUC1, a pro-invasive oncogene (*28*) that had been tentatively identified by microarray analysis to undergo suppression by **1** (*11*). Therefore, before beginning the testing of **3** and **4**, we first validated the effects of **1** on MUC1.

Verification of MUC1 Suppression. To validate MUC1 suppression as a legitimate end point for acylated ManNAc analogues, our first experiments verified the link between **1** and reduced MUC1 transcription. As shown in Figure 2, quantitative real-time PCR (qRT-PCR) and Western blot analysis both showed a dose-dependent decrease for MUC1 in MDA-MB-231 cells treated with **1**. In control experiments where *n*-butyrate was delivered via mannose (the hexose equivalent of ManNAc), the opposite effects, *i.e.*, potentiation of mRNA expression and increased protein levels, were observed for **2**. The significance of these results was several-fold. First, because MUC1 overexpression is strongly correlated with a highly invasive phenotype and poor prognosis and because small-molecule inhibitors of MUC1 have not been reported, **1** opens the door for a new class of therapeutic agents directed at this oncogene. More narrowly, the suppression of MUC1 by **1** provided an additional anticancer end point that complemented growth inhibition and cytotoxicity. Finally, the comparison of **1** and **2** reinforced the requirement, previously observed for apoptosis, for an *N*-acyl

group at the C2 position; because of the lack of bioactivity of **2**, hexoses were not further tested in this study.

Interestingly, the suppressive effects of **1** on MUC1 were not easily explained by the known biological activities of the SCFA (*n*-butyrate) and monosaccharide (ManNAc) components of the parent hybrid molecule. By contrast, the increase in MUC1 by **2** had precedent in a report where mucins were up-regulated by *n*-butyrate (*29, 30*). Therefore it is striking that **1**, which also liberates *n*-butyrate, reverses the potentiation of mucin expression, presumably through contributions of the core sugar ManNAc. Because there was no literature precedent for ManNAc having the capacity to alter transcription (*31*), the ability of **1** to reverse the transcriptional activation of MUC1 was initially puzzling. However, as became obvious in the SAR uncovered in subsequent sections of this report, **1** and other 6-*O*-SCFA-derivatized hexosamines have biological activities not accounted for by either the sugar or SCFA moieties. Instead, these molecules have a third modality where bioactivity is an inherent feature of an intact SCFA-sugar structure.

Decoupling Flux from Growth Inhibition. Upon establishing that three viable end points (growth inhibition, metabolic flux, and MUC1 suppression) existed for analogue evaluation, the testing of the tributanoylated compounds **3** and **4** commenced. A striking result from the initial comparison of **3** and **4** was that these two isomers had notably divergent biological activities. First, the C1-OH isomer **3** enhanced growth inhibition compared to perbutanoylated ManNAc **1** while metabolic flux and MUC1 suppression remained unchanged (Figure 3). At first the enhanced growth inhibition of **3**, presumed to result from HDACi activity of hydrolyzed *n*-butyrate and associated up-regulation of p21 (*11, 32*), was counterintuitive because a triacylated analogue delivers a lower molar ratio of SCFA (sialic acid production, which was identical for **1** and **3**, provided an internal control to ensure that ManNAc was being generated by **3**).

Remarkably, the C6-OH isomer **4** behaved dramatically differently. It had negligible cytotoxicity and enhanced rather than suppressed MUC1 while maintaining high flux through the sialic acid pathway up to concentrations where solubility became limiting (~400 μM; throughout this report testing was generally discontinued at the onset of toxicity *or* loss of solubility, and therefore comparisons of analogues plotted in the same graph often were done over different concentration ranges). An important ramification of these findings is that they unambiguously overturned the generally accepted premise that the biological activities of SCFA-monosaccharide hybrid molecules result from their constituent components after intracellular hydrolysis by nonspecific esterases (*i.e.*, **1**, **3**, and **4** would all be expected to increase sialic acid production due to ManNAc and inhibit proliferation due to the HDACi effects of *n*-butyrate (*11*)). Because **3** and **4** generate identical hydrolysis products, the distinct cellular responses to these compounds established a new paradigm where bioactivity is a property of hexosamine scaffolds with intact SCFA groups, which act as a unique class of pharmacophores (as discussed in Concluding Comments). Moreover, from a practical perspective, the finding that one isomer held properties favorable for cancer development (MUC1 suppression and enhanced cytotoxicity), while the other had characteristics favorable for glycan labeling (high flux with negligible growth inhibition), established SAR as valuable for separating the various conflicting biological activities required for different aspects of metabolic glycoengineering.

SAR Are General for SCFA-Hexosamines. As just described, the two tributyrate-derivatized ManNAc analogues demonstrated that the conflicting goals of anticancer activities (enhanced in the C1-OH analogue **3**) and flux (optimized in the C6-OH analogue **4**) could be separated by the regiospecific placement of *n*-butyrate on a ManNAc scaffold. To ascertain whether these SAR were unique to *n*-butyrate, which is highly active and described as the "SCFA par excellence" (*33*) or whether the SAR also apply to less active SCFAs such as acetate, we tested C1-OH (**6**) and C6-OH (**7**) triacetylated ManNAc analogues. In these experiments, neither compound efficiently supported flux into the sialic acid pathway compared to peracetylated ManNAc (**5**) (Figure 4). Interestingly, **6** was more growth inhibitory than the parent compound despite not activating sialic acid biosynthesis, whereas **7** had a negligible impact; these effects were consistent with the SAR set by the C1- and C6-OH tributanoylated analogues **3** and **4**. Moreover, MUC1 expression resulting from **6** and **7** followed the pattern set by **3** and **4** where the C1-OH analogue suppressed expression and the C6-OH analogue was mildly activating. These results established that the requirement of a C6-SCFA for toxicity and MUC1 suppression are not specific to butyrate but extend to other SCFAs including acetate.

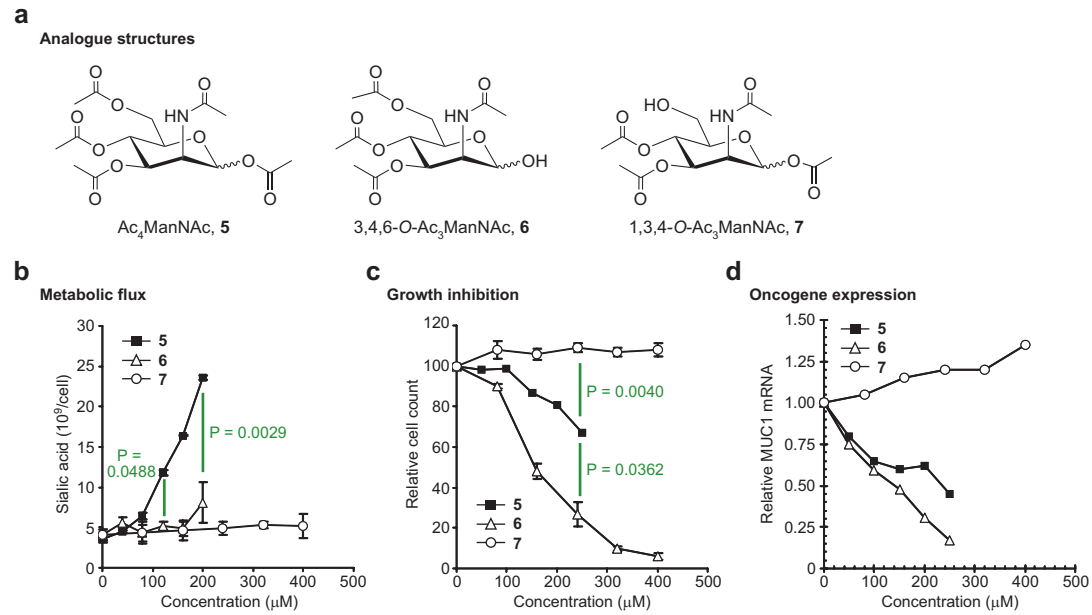

Figure 4. Bioactivities of peracetylated 5 and triacetylated ManNAc analogues 6 and 7 in MDA-MB-231 cells. a) Analogue structures. b) Metabolic flux determined by sialic acid production; only 5 increases flux with $p < 0.05$. c) Growth inhibition shows a stepwise significance between 7 (least toxic), 5 (intermediate), and 6 (greatest toxicity) at concentrations >240 μM. d) MUC1 mRNA levels determined by qRT-PCR. For b and c, error bars indicate SEM, $n \geq 3$, and data for a representative experiment, which was repeated three times, are shown for d.

The finding that 6-*O*-acetylated ManNAc shares cytotoxic and growth inhibitory properties with the butanoylated counterpart is significant because peracetylated analogues are widely used in metabolic glycoengineering (*4*) and, on the basis of the findings presented here, can explain the often-observed toxicity of these compounds. While usually not severely dose-limiting *in vitro* and infrequently observed *in vivo*, even negligible or latent toxicity is undesirable in glycan labeling experiments where artifacts could be introduced. Thus, the finding that C6-OH analogues virtually lack toxicity provides cleaner labeling agents. A drawback of the C6-OH triacetylated analogues, namely, poor membrane permeability, can be overcome by using *n*-butyrate as the SCFA; as shown in Figure 2 tributanoylated analogues are sufficiently lipophilic to support robust metabolic flux. Finally, the ability of **6** to inhibit the growth of cells at lower concentrations than required for flux provides another piece of evidence that sialic acid production is decoupled from analogue cytotoxicity, which instead occurs in response to specific placement of *n*-butyrate on ManNAc.

SAR of ManNAc analogues Extend to GlcNAc. In the next set of experiments, we further explored the importance of the stereochemistry of the *N*-acyl group of hexosamines to strengthen the developing hypothesis that the significant aspects of the bioactivity of 6-*O*-SCFA-derivatized ManNAc analogues lay outside of known sugar-specific mechanisms. Because ManNAc is a dedicated metabolic substrate for the sialic acid biosynthetic pathway with no other metabolic fates (*19*), we were interested in knowing whether equatorial stereochemistry of the *N*-acyl group, as found in GlcNAc analogues that do not activate sialic acid biosynthesis (*13*), would exhibit similar SAR. Therefore, the impact of the GlcNAc analogues **8**, **9**, and **10** (*i.e.*, the counterparts to ManNAc analogues **1**, **3**, and **4** but with equatorial *N*-acyl groups) were tested and found to follow the pattern set by the ManNAc analogues; data are shown for the Jurkat line in Figure 5 (similar results have been obtained for the MDA-MB-231 line, not shown). Specifically, the C1-OH derivative **9** was significantly more growth inhibitory than perbutanoylated GlcNAc (**8**) and the C6-OH derivative **10** had a negligible impact on proliferation.

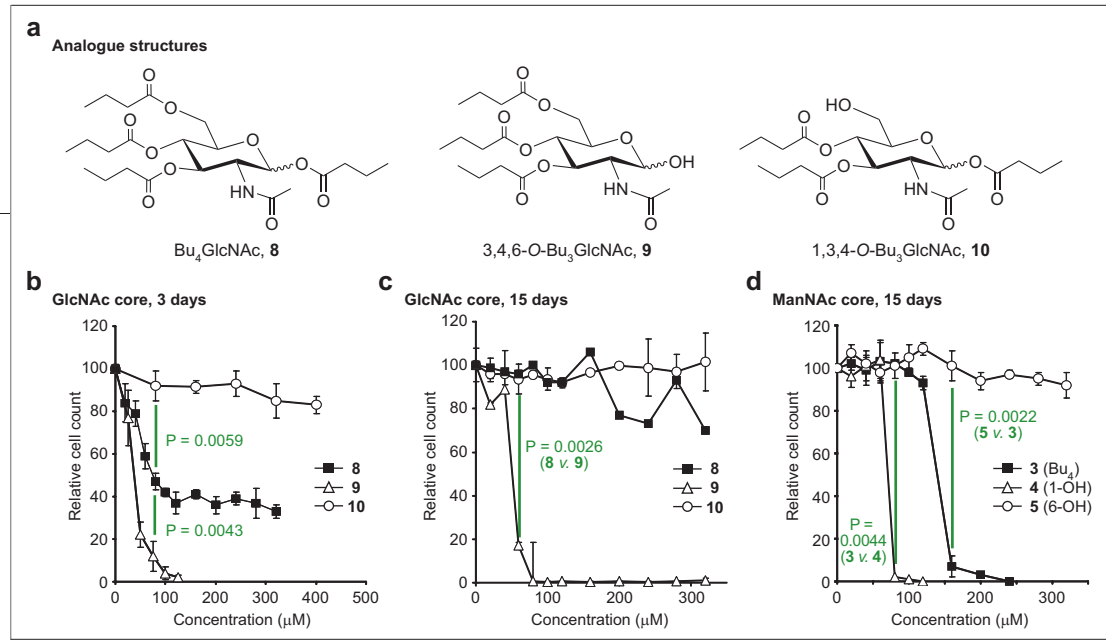

Figure 5. Growth inhibition and toxicity of butanoylated GlcNAc analogues in Jurkat cells. a) Analogue structures. b) Growth inhibition after 3 days of exposure to GlcNAc analogues showed a stepwise response where 10 had negligible impact, 8 had an intermediate effect, and 9 showed the greatest inhibition. c) After 15 days, only 9 was toxic (at concentrations >75 μM). d) Toxicity measurements after 15 days, for the comparable ManNAc analogues (*i.e.*, 3 ≈ 8, 4 ≈ 9, and 5 ≈ 10) showed that the per-butanolylated isomers had divergent activity (3 was toxic after 15 days but 8 was not) whereas the C1-OH and C6-OH tributanolyated analogues had similar effects. For b–d, error bars indicate SEM, $n \geq 3$.

The incubation of cells treated with the GlcNAc (Figure 5, panel c) or ManNAc (panel d) triacylated analogues for longer than 5 days further revealed the superior ability of either C1-OH analogue to inhibit cancer cells compared to their per- or C6-OH tributanoylated counterparts. This effect was particularly pronounced for GlcNAc where the perbutanoylated analogue provided a substantial degree of transient growth inhibition but cells recovered and resumed robust growth by 15 days. By contrast the initially growth-inhibited, C1-OH GlcNAc analogue-treated cells underwent apoptosis (which also occurred for all, *i.e.*, the per- and triacetylated and butanoylated, 6-*O*-SCFA ManNAc analogues tested, data not shown) after 15 days. There are several possible explanations for the differences between ManNAc and GlcNAc. The first option is that structural "cross-talk" exists between the C1 and C2 positions to tune the dominant response evoked by the SCFA derivatization at the C6 position. Another, nonexclusive, possibility is that sugar-specific metabolism can influence larger cellular responses in subtle ways; this premise is supported by the ability of ManNAc to alter sialic acid production and GlcNAc to impact *O*-GlcNAc protein signaling (*34, 35*). Finally, the ability of *n*-butyrate to selectively regulate the expression of glycosylation genes (*36*) indicates that a complex interrelated web of SCFA- and glycan-specific effects ultimately determines the exact bioactivity of any particular SCFA-hexosamine hybrid molecule.

SAR Apply to Glycan Labeling. Having demonstrated that *in vitro* anticancer attributes of the C1-OH derivatives of hexosamine-SCFA hybrids could be separated from metabolic flux, as well as enhanced, by analogue design, we next confirmed that the negligible toxicity of C6-OH regioisomers can be exploited to enhance glycan labeling. The impetus for these experiments came from the toxicity of analogues used in metabolic glycoengineering that hinders otherwise promising strategies for the labeling and visualization of glycans in living cells by bioorthogonal chemical approaches (*4, 23, 37*). Specifically, we explored whether the SAR determined with the naturally occurring hexosamines ManNAc and GlcNAc extended to abiotic monosaccharides by testing ManNAc analogues where the *N*-acyl position bore the levulinoyl ("Lev") group (*2, 13*). Of the many nonnatural functionalities appended to ManNAc analogues (*4*), the levulinoyl group was selected for two reasons. First, surface labeling and flow cytometry quantification of the glycocalyx-displayed ketone borne by this group provides a ready measurement of flux through the sialic acid pathway (Figure 6, panel a) (*16*). Second, in combination with peracetylation, the Lev group is highly toxic compared to other *N*-acyl modifications (*23*). Consequently we reasoned that if the SAR observed for the natural core sugars could ameliorate growth inhibition caused by the highly toxic Lev group, the same relationships would also apply to less cytotoxic *N*-acyl modifications.

Peracetylated ManNLev (**11**), a previously tested compound (*2, 13*), provided a baseline for the evaluation of perbutyrate- (**12**) and C6-OH tributyrate-modified (**13**) ManNLev (Figure 6, panel b). As predicted from the SAR shown in Figures 3–5, **13** was less growth inhibitory

(panel c) and supported higher surface labeling than either **11** or **12** (panel d). The surface ketone display supported by **13** was particularly noteworthy because the low analogue concentrations used (<20 μM) were in the subcytotoxic concentration range for **11** and **12**. The lower surface display resulting from the peracylated analogues, therefore, cannot be attributed entirely to the trivial explanation that flux was suppressed by growth inhibition (*18*). Instead, **13** had superior cell uptake, metabolic flux, and surface labeling characteristics in addition to negligible cytotoxicity. This result capped the SAR described in this report by establishing that "anticancer" properties of SCFA-hexosamines can be separated from metabolic flux not just for natural monosaccharides but also for core sugars bearing non-natural chemical groups used in metabolic glycoengineering.

Conclusion. The SAR described in this report represent a fundamental advance in the use of SCFA-hexosamine analogues for drug discovery and for efficient and safe metabolic substrates for glycan labeling via metabolic glycoengineering. These dual and often conflicting objectives were achieved by decoupling the biological activities required for each endeavor by describing the critical role of SCFA-derivatization of the C6-position of hexosamine scaffold. This discovery complements the recent flurry of chemistry-driven efforts (*38*) to exploit sugars as biocompatible, structurally rigid, three-dimensional, and surprisingly physiologically stable scaffolds for drug discovery (*39, 40*) in several important ways. First, the current results extend previous classes of carbohydrates such as hexoses, iminosugars, and disaccharides to now include hexosamines as an attractive sugar-based scaffold. Second, they provide carbohydrate-based libraries, which are in their early stages of development and remain in search of disease end points, with specific areas of biomedical significance that include apoptosis and suppression of pro-invasive oncogenes in human cancer cells for future study. Next, because structural features tune the bioactivity of C6-derivatized hexosamines (*e.g.*, ManNAc versus GlcNAc differences shown here in Figure 5 or the impact of the *N*-acyl substituent of peracetylated ManNAc analogues we showed previously (*23*)), combined with an increasing ability for selective acylation of monosaccharides (*41*) with a growing diversity of functional groups (*39*), the SAR described in this Article provide a rich starting point for broad range biological investigations and therapeutic interventions. Finally and most generally, the current SAR findings show that ester linkages in small molecule prodrugs, long exemplified by ester-linked acetate in acetyl salicylic acid that is hydrolyzed to generate the biologically active

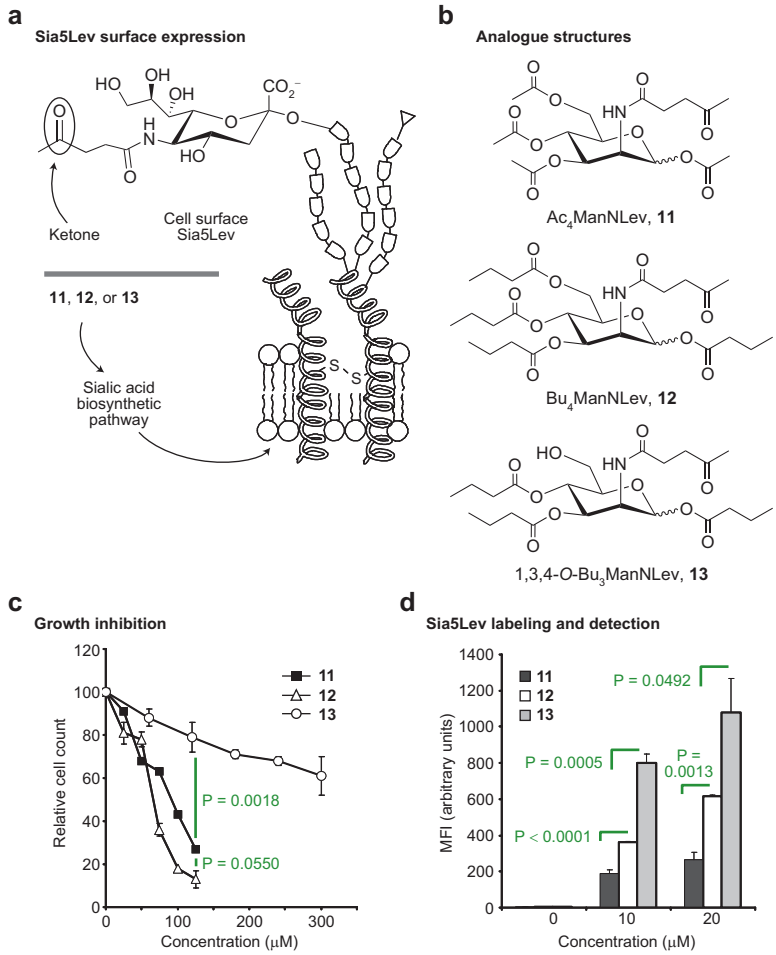

Figure 6. Surface expression of Sia5Lev in Jurkat cells. a) Sia5Lev is displayed in surface glycans upon biosynthetic incorporation of 11, 12, **and** 13 **(structures are shown in b). c) Growth inhibition after 3 days showed that the peracetyl-**11 **and perbutanoyl-**12 **ManNLev have equivalent effects, whereas the tributanoylated analogue** 13 **is significantly less inhibitory. d) Surface detection of ketone-bearing sialosides by conjugation with biotin hydrazide, staining with FITC-avidin, and quantification by flow cytometry showed that perbutanolylated ManLev (**12**) was more effective than the peracetylated analogue** 11**, and in turn, the C6-OH tributanolylated analogue (**13**) was more efficient than** 12**.**

form of aspirin, do not always require removal to generate biological activity. Instead, at least in the case of *n*-butyrate linked to hexosamines, these molecules have sufficient stability under physiological conditions to act as pharmacophores by virtue of intact HYBRID SCFA-monosaccharide linkages.

METHODS

Analogue Synthesis. The previously reported compounds **1**, **2**, **5**, **8**, and **11** were synthesized according to published methods (*11, 17, 23, 31*). The synthesis and characterization of **3**, **4**, **6**, **7**, **9**, **10**, **12**, and **13** are described in Supporting Information.

Cell Lines and Culture Conditions. The metastatic breast cancer MDA-MB-231 line was obtained from the ATCC and cultured in RPMI-1640 medium supplemented with 10% fetal bovine serum (FBS), glutamine, and penicillin/streptomycin according to the supplier's specifications. Jurkat (clone E-6) cells, also obtained from the ATCC, were cultured in RPMI-1640 medium supplemented with 5.0% FBS, glutamine, and penicillin/streptomycin. Cells were incubated at 37 °C in a water-saturated, 5.0% CO_2 incubator (*23*).

When testing cell responses to the SCFA-hexosamines, solutions of analogues in ethanol (or DMSO) were added to empty wells of tissue culture plasticware (typically, 6-well plates) in the appropriate amount to give concentrations ranges from 0 to 500 μM upon addition of cells and culture medium. Typically, the solvent was allowed to evaporate before the cells were added, leaving a thin coating of analogue on the well. Alternatively, the negative control and intermediate samples had an equivalent volume of ethanol (or DMSO) added as the highest concentration well (in all experiments the solvent volume was less than 0.8%). After the ethanol evaporated (typically in 5–10 min), MDA-MB-231 cells were plated at a density of 27,000 cells cm^{-2} in 6-well plates in 4.0 mL of medium per well, and suspension-grown Jurkat cells were seeded at a density of 2.5×10^5 cells mL^{-1}.

Analysis of MUC1 Expression by qRT-PCR. The expression of MUC1 was quantified by extracting mRNA from cells after 3 days of incubation with analogue by using Trizol (Invitrogen). The mRNA was treated with DNase (Ambion) to remove contaminating genomic DNA and purified using RNeasy spin columns (Qiagen). RNA quality was assessed with UV spectroscopy and agarose gel electrophoresis. For qRT-PCR, cDNA was obtained from the mRNA by using the SuperScript III First Stand synthesis kit (Invitrogen) and amplified in an ABI 7700 thermocycler using a SYBR green master mix (Applied Biosystems). MUC1 was amplified using the following primers: (FWD) 5′-AGACGTCAGCGTGAGT GATG-3′ and (REV) 5-GACAGCCAAGGCAATGAGAT-3′. GAPDH was used as the housekeeping gene for normalizing MUC1 expression. The following primers were used to amplify GAPDH: (FWD) 5′-CCACCCATGGCAAATTCC-3′ and (REV) 5′-GATGGGATTTC CATTGATGACA-3′. Validity of GAPDH as a housekeeping gene was confirmed by obtaining similar results using β-actin: (FWD) 5′-GCGGGAAATCGTGCGTGACATT-3′ and (REV) 5′-GATGGAGTTGA AGGTAGTTTCGTG-3′. All Ct values were measured in quadruplicate. Relative expression of MUC1 was calculated using average Ct values according to the $2^{-\Delta\Delta Ct}$ method (*42, 43*). Correct amplification was verified by agarose gel electrophoresis of the PCR products.

MUC1 Western Blotting. Whole cell lysates for Western blotting were obtained by washing cells twice in ice-cold PBS prior to lysis in RIPA buffer supplemented with a protease inhibitor cocktail (Sigma). An equal mass of protein was loaded into each well of a 4–20% SDS-PAGE gel based on protein quantification measurements obtained by using the BCA assay (Pierce Biotechnology). Following electrophoresis and blotting onto nitrocellulose, membranes were blocked in 5.0% milk in TBST for 1.0 h at RT, incubated with primary antibody overnight at 4.0 °C, incubated with HRP-conjugated secondary antibody (goat antimouse IgG, Santa Cruz Biotechnology) at a 1:25,000 dilution for 2.0 h at RT under constant agitation, and developed using a chemiluminescent reagent (Pierce Biotechnology, DuraWest SuperSignal). The murine monoclonal primary antibody used to detect MUC1 (Clone VU4H5, Santa Cruz Biotechnology) recognized the tandem repeat of the extracellular domain. Equal protein loading was confirmed using a monoclonal antibody for β-tubulin (Sigma).

Determination of Sialic Acid. A modification of the periodate-resorcinol assay (*18, 23*), originally described by Jourdian and co-workers (*44*), was used to measure production of sialic acid, typically 2 days after plating cells with analogue. Briefly, trypsinized cells were washed twice in PBS, counted using a Coulter Z2 electronic particle sizing instrument, and lysed during three freeze–thaw cycles. Lysates were oxidized with 0.4 M periodic acid, cooled on ice for 10 min, reacted with 500 μL of a freshly prepared resorcinol mixture (10% 0.5 M resorcinol, 10% 2.5 mM $CuSO_4$, 44% concentrated HCl, 36% deionized H_2O), and heated at 100 °C for 15 min. After cooling, 500 μL of *tert*-butyl alcohol was added, and optical density measurements at 630 nm were promptly recorded. The cellular content of sialic acid was calculated using the number of lysed cells and a calibration curve of authentic sialic acid (Pfanstiehl) simultaneously assayed alongside the samples.

Growth Inhibition and Toxicity. Growth inhibition was determined by trypsinizing the MDA-MB-231 cells 3 days after plating with analogues and then counting the cells by Coulter Z2 electronic particle sizing instrument. This assay provides a quantitative estimate of the growth inhibitory effects of analogue compared with untreated (*i.e.*, solvent vehicle) controls. Growth inhibition at 3 days (as reported for butyrate-ManNAc analogues in Figure 3, acetate-ManNAc analogues in Figure 4, butyrate-GlcNAc analogues in Figure 5, and SCFA-ManNLev analogues in Figure 6) has been studied extensively elsewhere by cell cycle progression indicative of HDACi effects, through live/dead cell assays, and by monitoring of apoptosis by caspase assays, DNA degradation, and Annexin V/PI flow cytometry analysis (*11, 23*), and results are in all cases consistent with the simplified analysis reported here. In addition, in some cases, depending on the specific structure of the analogue, growth-inhibited cells experience transient growth inhibition and later recover and resume robust growth. In other cases, growth-inhibited cells subsequently undergo apoptosis; a detailed explanation of the distinctions between growth inhibition and toxicity are provided in our prior publications (*11, 23*). Here, 15-day data were used to distinguish between short-term and long-term effects, as manifest for the perbutanoylated ManNAc and GlcNAc analogues **3** and **8**; Figure 5, panels c and d). When not explicitly shown, analogues that were efficient at inducing short-term growth inhibition (generally the peracyl and C1-OH triacyl compounds) led to long-term toxicity, whereas analogues with minimal growth inhibition, (*i.e.*, the C6-OH sugars) also had negligible long-term toxicity.

Quantification of Cell Surface Ketones. The detection and quantification of surface ketones upon incubation of Jurkat

cells with levulinoyl analogues **11**–**13** for 3 days followed published methods (*2*). Briefly, a biotinylated cross-linking agent containing a ketone-reactive hydrazide moiety was used to label the ketonized cell surface. The biotinylated cells were then stained with fluorescein-(FITC)-conjugated avidin and quantified by flow cytometry.

Supporting Information Available: This material is available free of charge *via* the Internet.

Acknowledgment: Funding was provided by the National Institutes of Health (CA112314-01A1 for ManNAc analogue synthesis and AR054005-01 for GlcNAc analogue synthesis) and by the Susan G. Komen Foundation (BCTR0503768) for MUC1 analysis.

REFERENCES

1. Kayser, H., Zeitler, R., Kannicht, C., Grunow, D., Nuck, R., and Reutter, W. (1992) Biosynthesis of a nonphysiological sialic acid in different rat organs, using *N*-propanoyl-D-hexosamines as precursors, *J. Biol. Chem. 267*, 16934–16938.
2. Mahal, L. K., Yarema, K. J., and Bertozzi, C. R. (1997) Engineering chemical reactivity on cell surfaces through oligosaccharide biosynthesis, *Science 276*, 1125–1128.
3. Saxon, E., and Bertozzi, C. R. (2000) Cell surface engineering by a modified Staudinger reaction, *Science 287*, 2007–2010.
4. Campbell, C. T., Sampathkumar, S.-G., Weier, C., and Yarema, K. J. (2007) Metabolic oligosaccharide engineering: perspectives, applications, and future directions, *Mol. Biosyst. 3*, 187–194.
5. Sawa, M., Hsu, T.-L., Itoh, T., Sugiyama, M., Hanson, S. R., Vogt, P. K., and Wong, C.-H. (2006) Glycoproteomic probes for fluorescent imaging of fucosylated glycans *in vivo*, *Proc. Natl. Acad. Sci. U.S.A. 103*, 12371–12376.
6. Agard, N. J., Baskin, J. M., Prescher, J. A., Lo, A., and Bertozzi, C. R. (2006) A comparative study of bioorthogonal reactions with azides, *ACS Chem. Biol. 1*, 644–648.
7. Keppler, O. T., Horstkorte, R., Pawlita, M., Schmidt, C., and Reutter, W. (2001) Biochemical engineering of the *N*-acyl side chain of sialic acid: biological implications, *Glycobiology 11*, 11R–18R.
8. Vocadlo, D. J., Hang, H. C., Kim, E.-J., Hanover, J. A., and Bertozzi, C. R. (2003) A chemical approach for identifying O-GlcNAc-modified proteins in cells, *Proc. Natl. Acad. Sc.i U.S.A. 100*, 9116–9121.
9. Sprung, R., Nandi, A., Chen, Y., Chan Kim, S., Barma, D., Falck, J. R., and Zhao, Y. (2005) Tagging-via-substrate strategy for probing O-GlcNAc modified proteins, *J. Proteome Res. 4*, 950–957.
10. Sampathkumar, S.-G., Li, A. V., Jones, M. B., Sun, Z., and Yarema, K. J. (2006) Metabolic installation of thiols into sialic acid modulates adhesion and stem cell biology, *Nat. Chem. Biol. 2*, 149–152.
11. Sampathkumar, S.-G., Jones, M. B., Meledeo, M. A., Campbell, C. T., Choi, S. S., Hida, K., Gomutputra, P., Sheh, A., Gilmartin, T., Head, S. R., and Yarema, K. J. (2006) Targeting glycosylation pathways and the cell cycle: sugar- dependent activity of butyrate-carbohydrate cancer prodrugs, *Chem. Biol. 13*, 1265–1275.
12. Liu, T., Guo, Z., Yang, Q., Sad, S., and Jennings, H. J. (2000) Biochemical engineering of surface α2,8 polysialic acid for immunotargeting tumor cells, *J. Biol. Chem. 275*, 32832–32836.
13. Yarema, K. J., Mahal, L. K., Bruehl, R. E., Rodriguez, E. C., and Bertozzi, C. R. (1998) Metabolic delivery of ketone groups to sialic acid residues. Application to cell surface glycoform engineering, *J. Biol. Chem. 273*, 31168–31179.
14. Sarkar, A. K., Fritz, T. A., Taylor, W. H., and Esko, J. D. (1995) Disaccharide uptake and priming in animal cells: inhibition of sialyl Lewis X by acetylated Gal β1,4GalcNAc β-*O*-naphthalenemethanol, *Proc. Natl. Acad. Sc.i U.S.A. 92*, 3323–3327.
15. Lemieux, G. A., Yarema, K. J., Jacobs, C. L., and Bertozzi, C. R. (1999) Exploiting differences in sialoside expression for selective targeting of MRI contrast reagents, *J. Am. Chem. Soc. 121*, 4278–4279.
16. Jacobs, C. L., Yarema, K. J., Mahal, L. K., Nauman, D. A., Charters, N., and Bertozzi, C. R. (2000) Metabolic labeling of glycoproteins with chemical tags through unnatural sialic acid biosynthesis, *Methods Enzymol. 327*, 260–275.
17. Jacobs, C. L., Goon, S., Yarema, K. J., Hinderlich, S., Hang, H. C., Chai, D. H., and Bertozzi, C. R. (2001) Substrate specificity of the sialic acid biosynthetic pathway, *Biochemistry 40*, 12864–12874.
18. Jones, M. B., Teng, H., Rhee, J. K., Baskaran, G., Lahar, N., and Yarema, K. J. (2004) Characterization of the cellular uptake and metabolic conversion of acetylated *N*-acetylmannosamine (ManNAc) analogues to sialic acids, *Biotechnol. Bioeng. 85*, 394–405.
19. Tanner, M. E. (2005) The enzymes of sialic acid biosynthesis, *Bioorg. Chem. 33*, 216–228.
20. Collins, B. E., Fralich, T. J., Itonori, S., Ichikawa, Y., and Schnaar, R. L. (2000) Conversion of cellular sialic acid expression from *N*-acetyl- to *N*-glycolylneuraminic acid using a synthetic precursor, *N*-glycolylmannosamine pentaacetate: inhibition of myelin-associated glycoprotein binding to neural cells, *Glycobiology 10*, 11–20.
21. Davie, J. R. (2003) Inhibition of histone deacetylase activity by butyrate, *J. Nutr. 133*, 2485S–2493S.
22. Basson, M. D., Liu, Y.-W., Hanly, A. M., Emenaker, N. J., Shenoy, S. G., and Gould Rothberg, B. E. (2000) Identification and comparative analysis of human colonocyte short-chain fatty acid response genes, *J. Gastrointest. Surg. 4*, 501–512.
23. Kim, E. J., Sampathkumar, S.-G., Jones, M. B., Rhee, J. K., Baskaran, G., and Yarema, K. J. (2004) Characterization of the metabolic flux and apoptotic effects of *O*-hydroxyl- and *N*-acetylmannosamine (ManNAc) analogues in Jurkat (human T-lymphoma-derived) cells, *J. Biol. Chem. 279*, 18342–18352.
24. Pan, Y., Chefalo, P., Nagy, N., Harding, C., and Guo, Z. (2005) Synthesis and immunological properties of *N*-modified GM3 antigens as therapeutic cancer vaccines, *J. Med. Chem. 48*, 875–883.
25. Sillanaukee, P., Pönnlö, M., and Jääskeläinen, I. P. (1999) Occurrence of sialic acids in healthy humans and different disorders, *Eur. J. Clin. Invest. 29*, 413–425.
26. Sampathkumar, S.-G., Campbell, C. T., Weier, C., and Yarema, K. J. (2006) Short-chain fatty acid-hexosamine cancer prodrugs: the sugar matters, *Drug Future 31*, 1099–1116.
27. Lipinski, C. A. (2004) Lead- and drug-like compounds: the rule-of-five revolution, *Drug Discovery Today Technol. 1*, 337–341.
28. Hattrup, C. L., and Gendler, S. J. (2006) MUC1 alters oncogenic events and transcription in human breast cancer cells, *Breast Cancer Res. 8*, R37.
29. Finnie, I. A., Dwarakanath, A. D., Taylor, B. A., and Rhodes, J. M. (1995) Colonic mucin synthesis is increased by sodium butyrate, *Gut 36*, 93–99.
30. Hatayama, H., Iwashita, J., Kuwajima, A., and Abe, T. (2007) The short chain fatty acid, butyrate, stimulates MUC2 mucin production in the human colon cancer cell line, LS174T, *Biochem. Biophys. Res. Commun. 356*, 599–603.
31. Sampathkumar, S.-G., Li, A. V., and Yarema, K. J. (2006) Synthesis of non-natural ManNAc analogues for the expression of thiols on cell surface sialic acids, *Nat. Protoc. 1*, 2377–2385.
32. Bai, L., and Merchant, J. L. (2000) Transcription factor ZBP-89 cooperates with histone acetyltransferase p300 during butyrate activation of p21(WAF1) transcription in human cells, *J. Biol. Chem. 275*, 30725–30733.
33. Roy, C. C., Kien, C. L., Bouthillier, L., and Levy, E. (2006) Short-chain fatty acids: Ready for prime time? *Nutr. Clin. Pract. 21*, 351–366.
34. Hanover, J. A. (2001) Glycan-dependent signaling: O-linked *N*-acetylglucosamine, *FASEB J. 15*, 1865–1876.
35. Zachara, N. E., and Hart, G. W. (2004) O-GlcNAc a sensor of cellular state: the role of nucleocytoplasmic glycosylation in modulating cellular function in response to nutrition and stress, *Biochim. Biophys. Acta 1673*, 13–28.

36. Radhakrishnan, P., Beum, P. V., Tan, S., and Cheng, P. W. (2007) Butyrate induces sLex synthesis by stimulation of selective glycosyltransferase genes, *Biochem. Biophys. Res. Commun. 359*, 457–462.
37. Hsu, T.-L., Hanson, S. R., Kishikawa, K., Wang, S.-K., Sawa, M., and Wong, C.-H. (2007) Alkynyl sugar analogues for the labeling and visualization of glycoconjugates in cells, *Proc. Natl. Acad. Sci. U.S.A. 104*, 2614–2619.
38. Jain, R. K., Kamau, M., Wang, C., Ippolito, R., Wang, H., Dulina, R., Anderson, J., Gange, D., and Sofia, M. J. (2003) 3-Azido-3-deoxyglycopyranoside derivatives as scaffolds for the synthesis of carbohydrate-Based universal pharmacophore mapping libraries, *Bioorg. Med. Chem. Lett. 13*, 2185–2189.
39. Meutermans, W., Le, G. T., and Becker, B. (2006) Carbohydrates as scaffolds in drug discovery, *ChemMedChem 1*, 1164–1194.
40. Barchi, J., Jr (2000) Emerging role of carbohydrates and glycomimetics in anticancer drug design, *Curr. Pharm. Des. 6*, 485–501.
41. Kawabata, T., Muramatsu, W., Nishio, T., Shibata, T., and Schedel, H. (2007) A catalytic one-step process for the chemo- and regioselective acylation of monosaccharides, *J. Am. Chem. Soc. 129*, 12890–12895.
42. Livak, K. J., and Schmittgen, T. D. (2001) Analysis of relative gene expression data using real-time quantitative PCR and the $2^{-\Delta\Delta CT}$ method, *Methods 25*, 402–408.
43. Wang, Z., Sun, Z., Li, A. V., and Yarema, K. J. (2006) Roles for GNE outside of sialic acid biosynthesis: modulation of sialyltransferase and BiP expression, GM3 and GD3 biosynthesis, proliferation and apoptosis, and ERK1/2 phosphorylation, *J. Biol. Chem. 281*, 27016–27028.
44. Jourdian, G. W., Dean, L., and Roseman, S. (1971) The sialic acids. XI. A periodate-resorcinol method for the quantitative estimation of free sialic acids and their glycosides, *J. Biol. Chem. 246*, 430–435.